Supporting Information

Narayanaswamy et al. 10.1073/pnas.0812771106

SI Materials and Methods

Media and Yeast Strains. Yeast strains with genetic background EY0986 (ATCC 201388: *MATa his3Δ1 leu2Δ0 met15Δ0 ura3Δ0* (S288C)) or BY4741 [genotype, *MATa his3Δ1 leu2Δ0 met15Δ0 ura3Δ0*] were used for all experiments. Rich (YPD) medium contained Yeast Extract (1%), Peptone (2%) and glucose (2%). Synthetic medium contained 1x Yeast Nitrogen Base (YNB; BD Biosciences/Difco) without amino acids, synthetic drop-out medium supplement mix (US Biosciences) and glucose (2%). Synthetic complete medium (SC) was synthetic medium supplemented with all amino acids and other supplements as described in ref. 1. Synthetic adenine dropout medium (SC-Adenine) was SC lacking adenine. Synthetic glucose dropout medium (SC-Glucose) was SC lacking glucose. Synthetic minimal medium (SD) was synthetic medium with only the supplements necessary for auxotrophic growth (leucine, methionine and uracil). Synthetic medium without a nitrogen source (SD-N) was SD with 1× YNB lacking ammonium sulfate and amino acids (BD Biosciences/Difco). All deletion strains were obtained from the Invitrogen BY4741 haploid deletion collection and were grown in the presence of the selective antibiotic G418.

Introduction of fluorescent protein epitope-tags into wild-type, TAP-tagged, or deletion strains was carried out using the method of Longtine et al. (2). The Longtine carboxyl-terminal GFP-tagging plasmid pFA6a-GFPS65T-HIS3MX6 (provided by the laboratory of Makkuni Jayaram, University of Texas) was used for the introduction of GFP-tags. Epitope-tagged strains were verified by colony PCR after growth on selective media. YFP and CFP fusion plasmids, pDH6 and pDH3, respectively (provided by the Yeast Resource Center, University of Washington), were used to introduce carboxyl-terminal yellow fluorescent protein (YFP) fusions to the GLN1 or ADE4 genes, and cyan flourescent protein (CFP) fusions to PHO88 and DCP2, respectively, for colocalization studies (Figs. S1 and Figs. S2). For colocalization with the nucleus and vacuole, cells were imaged after addition of DAPI stain (Vector Labs) or 80 μM FM4–64 dye (Molecular Probes), respectively. For colocalization with actin bodies, cells were fixed by incubation with 4% formaldehyde at room temperature for 20 min, washed 3 times with PBS, incubated with 1/50th, 1/20th, or 1/10th the volume of Alexa Fluor 647 Phalloidin (Invitrogen) for 1 h at room temperature, washed 3 times with PBS and then imaged.

High-Throughput Imaging by Cell Microarrays. Spotted cell microarrays (3) were manufactured from the *S. cerevisiae* GFP-tagged yeast strain collection (4) (Invitrogen). The collection was based on strain EY0986, and each of ≈4,200 individual strains was chromosomally tagged with the coding sequence of *Aequorea victoria* GFP (S65T) at the C terminus of an ORF (4). This collection was replicated in 96-well plates, using a Biomek FX liquid handling robot. Each strain was inoculated into 200 μL of YPD containing 17% glycerol, grown at 30 °C for ≈2 days without shaking, mixed on a plate shaker, and sealed and frozen at −80 °C.

A copy of the GFP clone collection was thawed and used to seed YPD medium (1:100 dilution). After growth to near saturation for ≈36 h at 30 °C, a second dilution (1:100) into YPD was carried out. This culture (twice removed from the original glycerol stock) was grown to stationary phase for 5 days at 30 °C and then fixed with 1% formaldehyde for 1 h. The fixed strains were washed 3 times with 1 x PBS to remove excess fixative, and resuspended in 1× PBS with 17% glycerol. These sample plates were directly printed onto slides, or stored at −80 °C and later printed.

Cell microarrays were printed onto freshly treated polyL-lysine coated slides via contact deposition of a fixed suspension, using a DNA microarray spotting robot. Slides were scanned using a GenePix microarray scanner to identify the locations of cell spots, and the cells in each spot were then finely imaged using an automated Nikon E800 fluorescence microscope and Photometrix Coolsnap CCD camera as in (3). DIC images and fluorescent images in the DAPI and GFP channels (measuring emission at 475 nm and 535 nm, respectively) were collected from each spot on 2 replicate slides, for a total of ≈26,000 microscope images. Images were stored and analyzed using the Cellma cell microarray image database software (3). Two independent graders manually inspected the images from the GFP-tagged strains that had previously been annotated as localized to the cytoplasm (4). Graders selected those strains in which the GFP-fusion protein showed a punctate localization in at least several cells in the field.

Confirmation of Foci Formation by Immunofluorescence. TAP-tagged yeast strains (Open Biosystems) were grown at 30 °C in YPD or appropriate dropout medium, to mid-log or stationary phase, as appropriate. Cells were fixed by adding glutaraldehyde to a final concentration of 2 or 4% and incubating on ice for 2 h, followed by 3 washes in 1× PBS solution. Cells were spheroplasted using 0.2 mL of 25 ng/mL Zymolase 20T (Seikagaku Corp.) and 2 μL/mL 2-mercaptoethanol in 1.2 M sorbitol and 0.1 M potassium phosphate buffer at pH 7. After washing in spheroplasting buffer, cells were spotted onto L-lysine coated Superfrost Plus slides (Fisher) and incubated in 3% BSA in 1x phosphate buffer saline solution for 30 min at 30C to block nonspecific binding sites. Slides were washed in 1× PBS, incubated for 2 h at 30 °C with FITC-conjugated rabbit anti-goat IgG (Zymed) at a 1:500 dilution in blocking buffer, then imaged.

Biochemical Fractionation of Gln1-GFP Punctate Bodies. Biochemical fractionation of Gln1-GFP punctate bodies was done by a modification of the protocol used by Teixeira et al. (5). Briefly, cells were grown in YPD for 48 h and harvested by centrifugation. A portion of the punctate body-containing sample was cycled to the diffuse state by adding fresh YPD to the cell pellet and shaking at 30 °C for 2 h, and then harvested by centrifugation. Both samples were washed in cold lysis buffer (50 mM Tris pH 7.6, 50 mM NaCl, 5 mM $MgCl_2$, 1 mM 2-mercaptoethanol, and 1x Roche EDTA-free protease inhibitor mixture) without detergents and lysed using glass beads. Lysis was >90% as determined by microscopic examination. Separation into supernatant and pellet fractions was carried out by centrifugation at 10,000 × *g* for 10 min.

Ficoll Gradient Fractionation of Gln1-GFP Punctate Bodies. Discontinuous Ficoll gradient fractionation of Gln1-GFP punctate bodies was performed using a modified version of the vacuole purification protocol from Reider and Emr (6). Briefly, Gln1-GFP tagged *S. cerevisiae* were grown in YPD for 48 h and harvested by centrifugation. Punctate body formation was confirmed by microscopy. Cells were suspended in a mixture of Roche EDTA-free protease inhibitor and gradient buffer (34 mM imidazole, pH 7.1, 60 mM $MgCl_2$, 19 mM KCl, and 45 mM ammonium chloride), and then lysed using glass beads. Lysis was confirmed by microscopy. 48 μg/mL (final concentration) of

DEAE Dextran (Sigma) was added to 500 μL of lysed cells (a total of 25 mL of ≈8 OD_{600} cells) and then loaded onto a layer of 2.9 mL of 16% (wt/vol) Ficoll solution in gradient buffer in an ultracentrifugation tube (Beckman). 3 mL of 8% (wt/vol) Ficoll in gradient buffer, 4 mL of 4% Ficoll (wt/vol) in gradient buffer, and 2 mL of gradient buffer were layered, respectively, onto the cell lysate. Additional gradient buffer was added as needed to balance the ultracentrifugation tubes. The density of the concentrated protein sample plus DEAE Dextran was difficult to predict in advance, and some mixing of the cell lysate with Ficoll layers was noted (although this did not affect the ultimate result, the pelleting of the punctate bodies). Gradients were centrifuged at 30,000 rpm in a Beckman SW41 rotor for 1.5 h at 8° Celsius. One-milliliter fractions were taken from the top of the gradient, leaving ≈1.5 mL for the final liquid fraction, 12. The pellet at the bottom of the gradient (fraction 13) was then suspended in 150 μL of PBS and clarified in a minicentrifuge for 30 seconds at ≈6,000 rpm.

Western blots with purified GFP standards (minimum of 4) were used to quantitate the GFP in Ficoll gradient fractions (triplicate measurements). Briefly, 4 μL of 4× NuPAGE LDS dye (Invitrogen) was added to 10 μL of a Ficoll gradient fraction or diluted fraction. Samples and GFP standards (Millipore) were denatured for 10 min at 70° Celsius and run on 4–12% NuPAGE BisTris gels (Invitrogen). Gels were transferred to 0.45 μm nitrocellulose membrane (Invitrogen), using the XCell II Blot transfer apparatus (Invitrogen). Blots were blocked with Odyssey Blocking Buffer (LI-COR) and then incubated with rabbit anti-GFP antibody (Sigma) for 2 h at room temperature or overnight at 4° Celsius. Blots were washed 3 times with PBST (PBS with 0.05% (vol/vol) Tween) and then incubated for 1 h with a secondary antibody (Odyssey goat anti-rabbit IR dye 680 antibody conjugate (LI-COR)). Again, blots were washed 3 times with PBST, and finally scanned using the LI-COR Odyssey Imaging System. GFP was quantified using the instrument's image analysis software.

Foci in the Ficoll gradient fractions and the clarified pellet fraction were quantitated using the previously described fluorescence microscope and camera. Size and fluorescence intensity criteria for the isolated protein aggregates were established based on the known cellular Gln1-GFP foci. In particular, cellular bodies were found to be ≈1 μm in size, and had a fluorescence intensity greater than or equal to ≈400 grayscale (MetaMorph version 6.2r6). The average density of punctate bodies was determined for each fraction. Punctate bodies were counted from 45 images (870 × 650 μm^2 per image) taken from a 22 × 22 mm^2 area over which 5 μL of a Ficoll fraction was spread.

Mass Spectrometry Based Validation of Punctate Formation. Foci formation and dissolution to the diffuse state were verified with an epitope-tag independent, mass spectrometry-based approach (Fig. 5). Briefly, *S. cerevisiae* strain BY4741 was grown in duplicate in YPD medium to stationary phase (3 days). One of the cultures (termed the "recovered" culture) was pelleted and resuspended in fresh YPD for 2 h with shaking at 30 °C. Samples with approximately equal numbers of cells were separated into pellet and supernatant fractions, as described above.

All 4 resulting samples (supernatant and pellet fractions from stationary and recovered phases; referred to as S_{sup}, S_{pel}, R_{sup}, R_{pel}, respectively) were treated with the acid-labile surfactant, Rapigest SF (Waters Inc.) to facilitate denaturation. Briefly, the pellet and supernatant fractions were incubated in lysis buffer containing 0.1% Rapigest SF in 50 mM $(NH_4)_2CO_3$, 5 mM DTT, and heated at 60 °C for 30 min. The samples were cooled to room temperature and protein concentrations estimated using the BCA protein assay kit (Pierce 23252). Protein samples were adjusted to 2 mg/mL each and the sulfhydryl groups alkylated by adding iodoacetamide to a final concentration of 55 mM followed by incubation in the dark for 30 min. Trypsin digestion was carried out using 1:20 wt/wt sequencing grade trypsin (Sigma) followed by overnight incubation at 37 °C. After digestion, trifluoroacetic acid (TFA) was added to a final concentration of 0.5% (pH <2). The samples were incubated at 37 °C for 30–45 min and centrifuged at 10,000 × *g* for 10 min. Samples were lyophilized, resuspended in 95% water/5% acetonitrile (ACN)/0.1% formic acid and passed through a YM-10 Microcon filter (Millipore).

Mass spectrometry (MS) of the resultant tryptic peptides was performed essentially as described in Lu et al. (7). Briefly, tryptic peptide mixtures were separated by automated 2-dimensional high performance liquid chromatography before MS analysis. Sample loading and strong cation exchange chromatography was performed at 2 μL/min; reverse phase chromatography was performed at 200–400 nL/min, with all buffers acidified with 0.1% formic acid. A BioBasic-SCX 100 × 0.18 (mm) column was used for first dimensional peptide separation. Fractions were eluted from the strong cation exchange column with a continuous 5% ACN background and progressive 5-min applications of 0, 20, 100 and 900 mM ammonium chloride. Each salt "bump" was eluted directly onto a reverse-phase C8 trap cartridge and washed free of salt, then eluted onto a reverse phase C18 column. Reverse-phase chromatography involved a 95-min gradient from 5% to 50% ACN, then a 25-min gradient from 50% to 95% ACN. Peptides were analyzed online via electrospray ionization ion trap mass spectrometry on a ThermoFinnigan Surveyor/LTQ-Orbitrap instrument. In each MS spectrum, the 7 tallest individual peaks in the mass/charge range 300-1500 *m/z* were fragmented by collision-induced dissociation (CID) with helium gas to produce MS/MS spectra.

Proteins were identified from a database of all nondubious ORF yeast protein sequences (8) using the program BioWorks TurboSequest 3.2 (ThermoFinnigan), considering up to 2 missed tryptic cleavages, followed by analysis by PeptideProphet (9) and ProteinProphet (10). A total of 1,605 proteins were identified in at least 1 of the 4 samples at a 5% false discovery rate, estimated using the ProteinProphet error model.

Protein Quantitation in Soluble and Insoluble Subcellular Fractions. To measure the relative enrichment of each protein *i* between the soluble and insoluble cell fractions, we used the differential Absolute Protein EXpression measurement (APEX) technique (7, 11): We counted the number n_i of observed MS/MS spectra associated with each identified protein *i* from a given cell fraction and calculated relative protein abundance f_i for that fraction as $f_i = n_i/N$, where N is the total number of interpreted MS/MS spectra obtained from that cell fraction (ranging here from 12,081 to 17,929 spectra). Based on these measures of f_i, the differential protein enrichment (i.e., bias toward either the soluble or insoluble protein fraction) was calculated using a Z score as

$$Z = \frac{f_{i,\mathrm{sup}} - f_{i,\mathrm{pel}}}{\sqrt{f_{i,0}(1 - f_{i,0})/N_{\mathrm{sup}} + f_{i,0}(1 - f_{i,0})N_{\mathrm{pel}}}}$$

where the numerator represents the difference in sampled proportions of protein *i* in the soluble (*sup*) and insoluble (*pel*) protein shotgun proteomics experiments $f_{i,\mathrm{sol}} = n_{i,\mathrm{sol}}/N_{\mathrm{sol}}$, $f_{i,\mathrm{pel}} = n_{i,\mathrm{pel}}/N_{\mathrm{pel}}$; and the denominator represents the standard error of the difference under the null hypothesis in which the 2 sampled proportions are drawn from the same underlying distribution with the overall proportion,

$$f_{i,0} = \frac{n_{i,\mathrm{sol}} + n_{i,\mathrm{pel}}}{N_{\mathrm{sol}} + N_{\mathrm{pel}}}.$$

Proteins with $Z \geq 1.96$ (less than or equal to -1.96) were judged to be significantly enriched in the soluble (insoluble) fraction at the 95% confidence level. As an example, 144 MS/MS spectra were observed from the protein Pma1p in the stationary phase pellet ($n_{i,\mathrm{pel}} = 144$); in contrast, no MS/MS spectra were observed for Pma1p in the stationary phase soluble fraction ($n_{i,\mathrm{sup}} = 0$), corresponding to $Z(S_{\mathrm{sup}}\text{–}S_{\mathrm{pel}}) = -10.24$, indicating a highly statistically significant enrichment of Pma1p in the insoluble fraction, consistent with its role as the major plasma membrane H^+-ATPase in yeast. In contrast, 52 MS/MS spectra were attributable to the protein Ald6p in the soluble stationary phase fraction, versus 4 MS/MS spectra in the insoluble stationary phase fraction, corresponding to a $Z(S_{\mathrm{sup}}\text{–}S_{\mathrm{pel}}) = 7.71$, indicating a highly significant bias toward the soluble fraction, consistent with the known role of Ald6 as a cytosolic aldehyde dehydrogenase.

Z scores were then analyzed as described in the main text.

1. Burke D, Dawson D, Stearns T (2000) *Methods in Yeast Genetics: A Cold Spring Harbor Laboratory Course Manual* (Cold Spring Harbor Laboratory Press, Cold Spring Harbor, NY).
2. Longtine MS, et al. (1998) Additional modules for versatile and economical PCR-based gene deletion and modification in Saccharomyces cerevisiae. *Yeast* 14:953–961.
3. Narayanaswamy R, et al. (2006) Systematic profiling of cellular phenotypes with spotted cell microarrays reveals mating-pheromone response genes. *Genome Biol* 7:R6.
4. Huh WK, et al. (2003) Global analysis of protein localization in budding yeast. *Nature* 425:686–691.
5. Teixeira D, Sheth U, Valencia-Sanchez MA, Brengues M, Parker R (2005) Processing bodies require RNA for assembly and contain nontranslating mRNAs. *RNA* 11:371–382.
6. Rieder SE, Emr SD (2001) Isolation of subcellular fractions from the yeast Saccharomyces cerevisiae. *Curr Protoc Cell Biol* Chapter 3:Unit 3 8.
7. Lu P, Vogel C, Wang R, Yao X, Marcotte EM (2007) Absolute protein expression profiling estimates the relative contributions of transcriptional and translational regulation. *Nat Biotechnol* 25:117–124.
8. Christie KR, et al. (2004) Saccharomyces Genome Database (SGD) provides tools to identify and analyze sequences from Saccharomyces cerevisiae and related sequences from other organisms. *Nucleic Acids Res* 32:D311–D314.
9. Keller A, Nesvizhskii AI, Kolker E, Aebersold R (2002) Empirical statistical model to estimate the accuracy of peptide identifications made by MS/MS and database search. *Anal Chem* 74:5383–5392.
10. Nesvizhskii AI, Keller A, Kolker E, Aebersold R (2003) A statistical model for identifying proteins by tandem mass spectrometry. *Anal Chem* 75:4646–4658.
11. Lu P, et al. (2007) Global metabolic changes following loss of a feedback loop reveal dynamic steady states of the yeast metabolome. *Metab Eng* 9:8–20.
12. Guldener U, et al. (2005) CYGD: The Comprehensive Yeast Genome Database. *Nucleic Acids Res* 33:D364–D368.
13. Robinson MD, Grigull J, Mohammad N, Hughes TR (2002) FunSpec: A web-based cluster interpreter for yeast. *BMC Bioinformatics* 3:35.

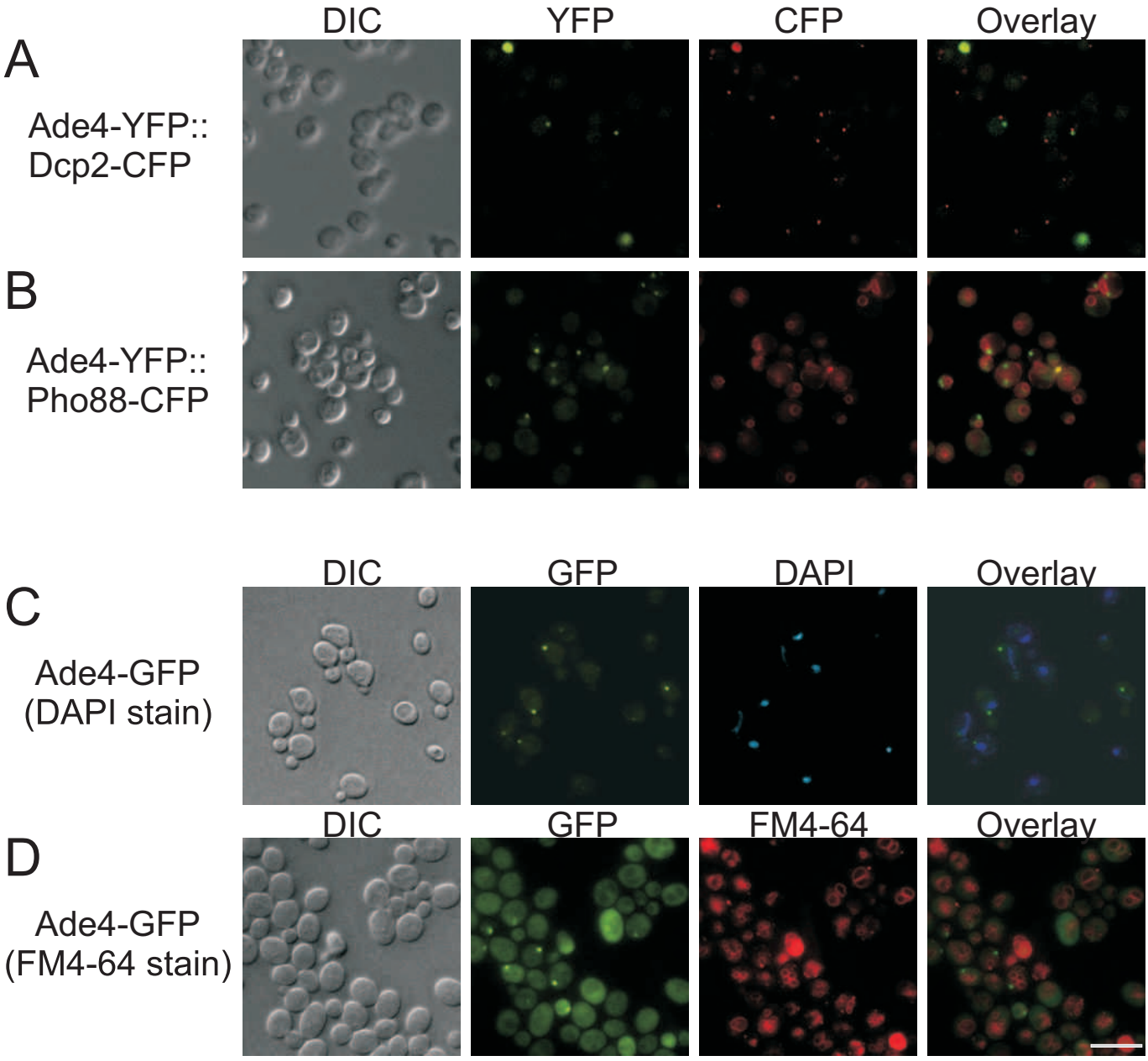

Fig. S1. Ade4 punctate foci do not colocalize with the nucleus, endoplasmic reticulum, vacuoles, or P-bodies. Ade4-YFP fails to colocalize with (*A*) the cyan fluorescent protein (CFP)-tagged P-body marker Dcp2-CFP, or with (*B*) the CFP-tagged endoplasmic reticulum marker Pho88-CFP. Ade4-GFP fails to colocalize with (*C*) the nucleus, as stained by DAPI dye, or with (*D*) vacuoles, as stained by FM4–64. *A* and *B* were performed on Ade4 punctate foci induced in SC stationary phase (48 h); *C* and *D* were performed on Ade4 punctate foci induced in SC-adenine dropout medium. (Scale bar: 10 μm.)

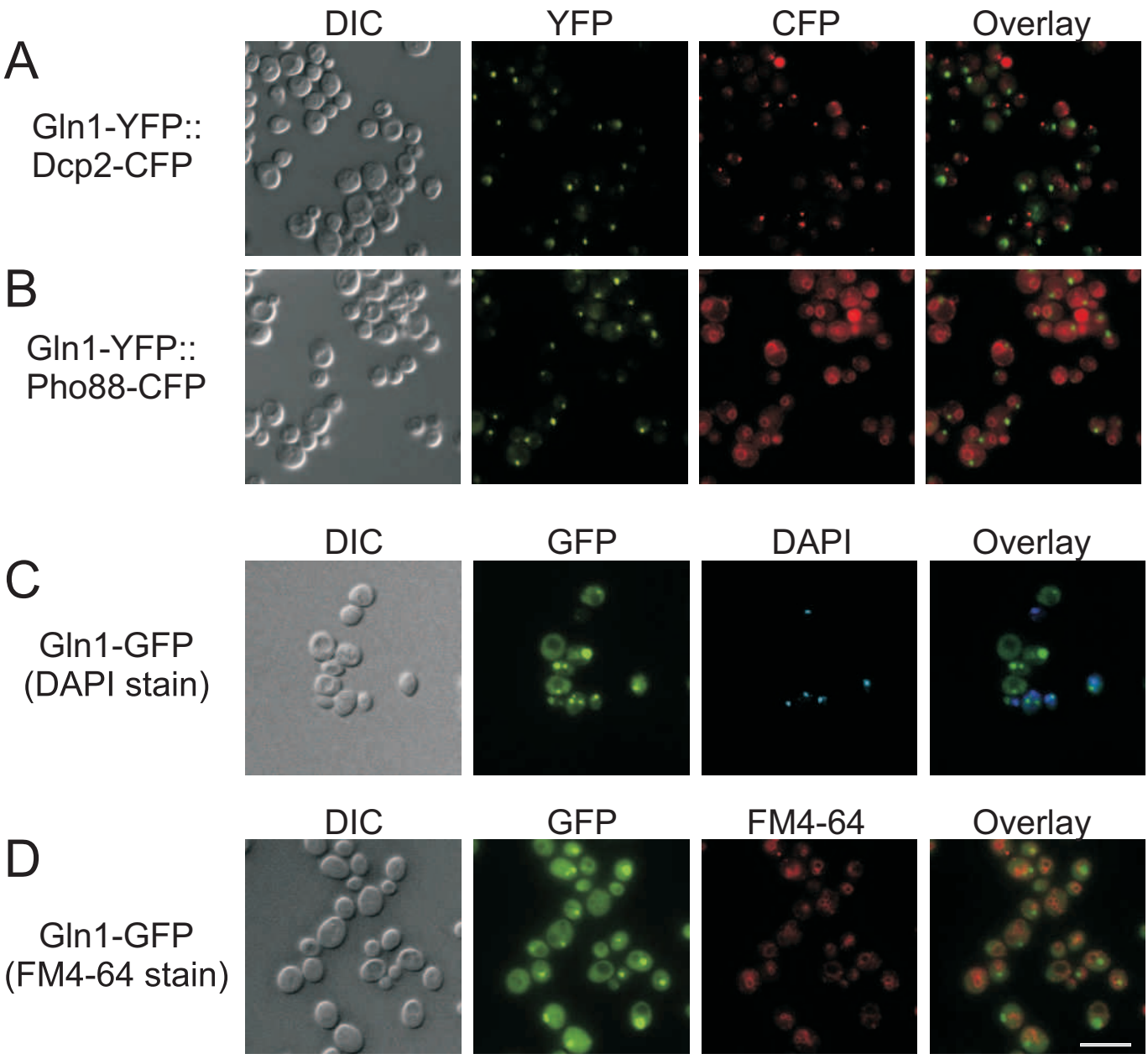

Fig. S2. Gln1 punctate foci do not colocalize with the nucleus, endoplasmic reticulum, vacuoles, or P-bodies. Gln1-YFP fails to colocalize with (*A*) the cyan fluorescent protein-tagged P-body marker Dcp2-CFP or with (*B*) the CFP-tagged endoplasmic reticulum marker Pho88-CFP. Gln1-GFP fails to colocalize with (*C*) the nucleus, as stained by DAPI dye, or with (*D*) vacuoles, as stained by FM4–64. *A* and *B* were performed on Gln1 punctate foci induced in SC stationary phase (48 h); *C* and *D* were performed on Gln1 punctate foci induced in SC-glucose dropout medium. (Scale bar: 10 μm.)

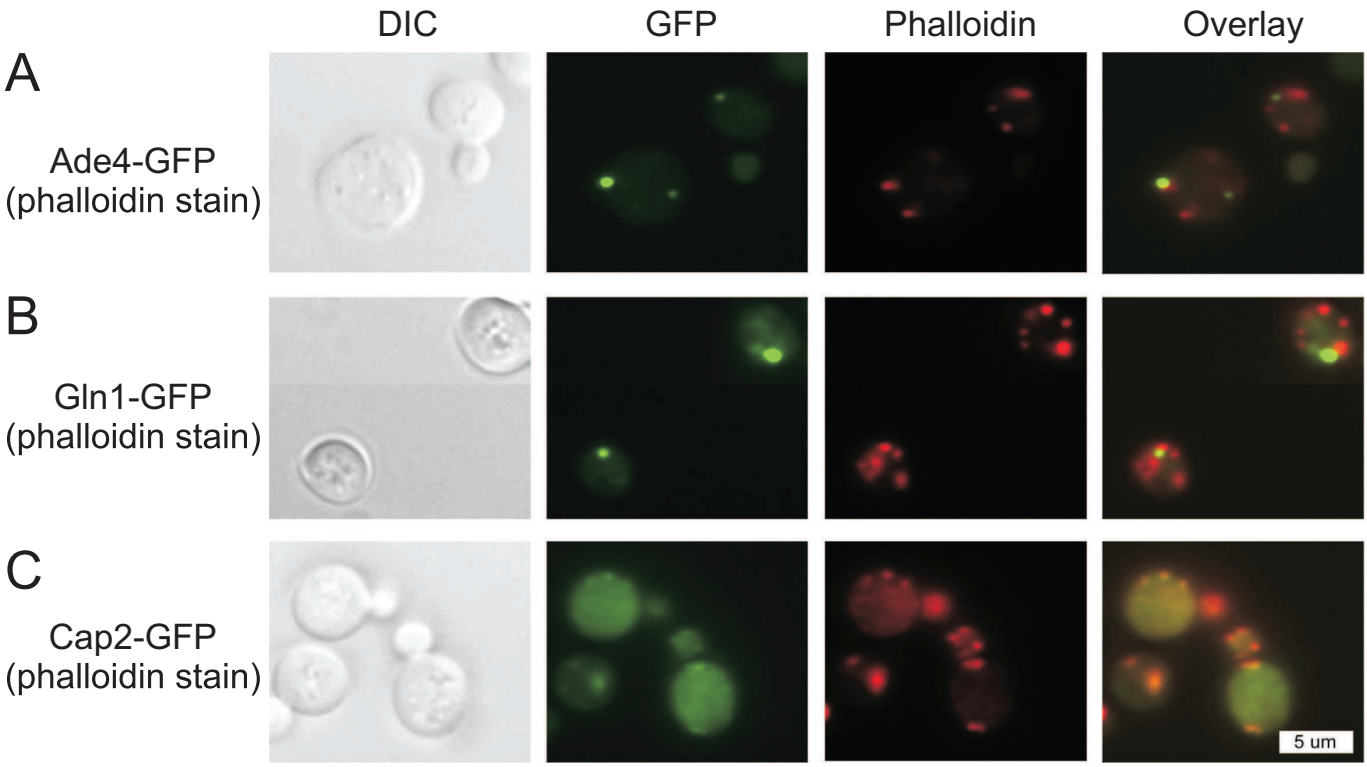

Fig. S3. Ade4 and Gln1 punctate foci do not strongly colocalize with actin bodies, unlike positive control marker Cap2, as detected by counter staining of stationary phase cells expressing Ade4-GFP, Gln1-GFP or Cap2-GFP by Alexa-Fluor 647-conjugated phalloidin. Punctate foci were induced in SC medium by growing to stationary phase (56 h). Ade4-GFP and Gln1-GFP punctate foci were fully colocalized with actin bodies in 12% and 4% of cases, respectively, in contrast to Cap2-GFP, which colocalized with actin bodies in 94% of cases (analyzing $n = 51$, 53, and 90 punctate foci, respectively). (Scale bar: 5 μm.)

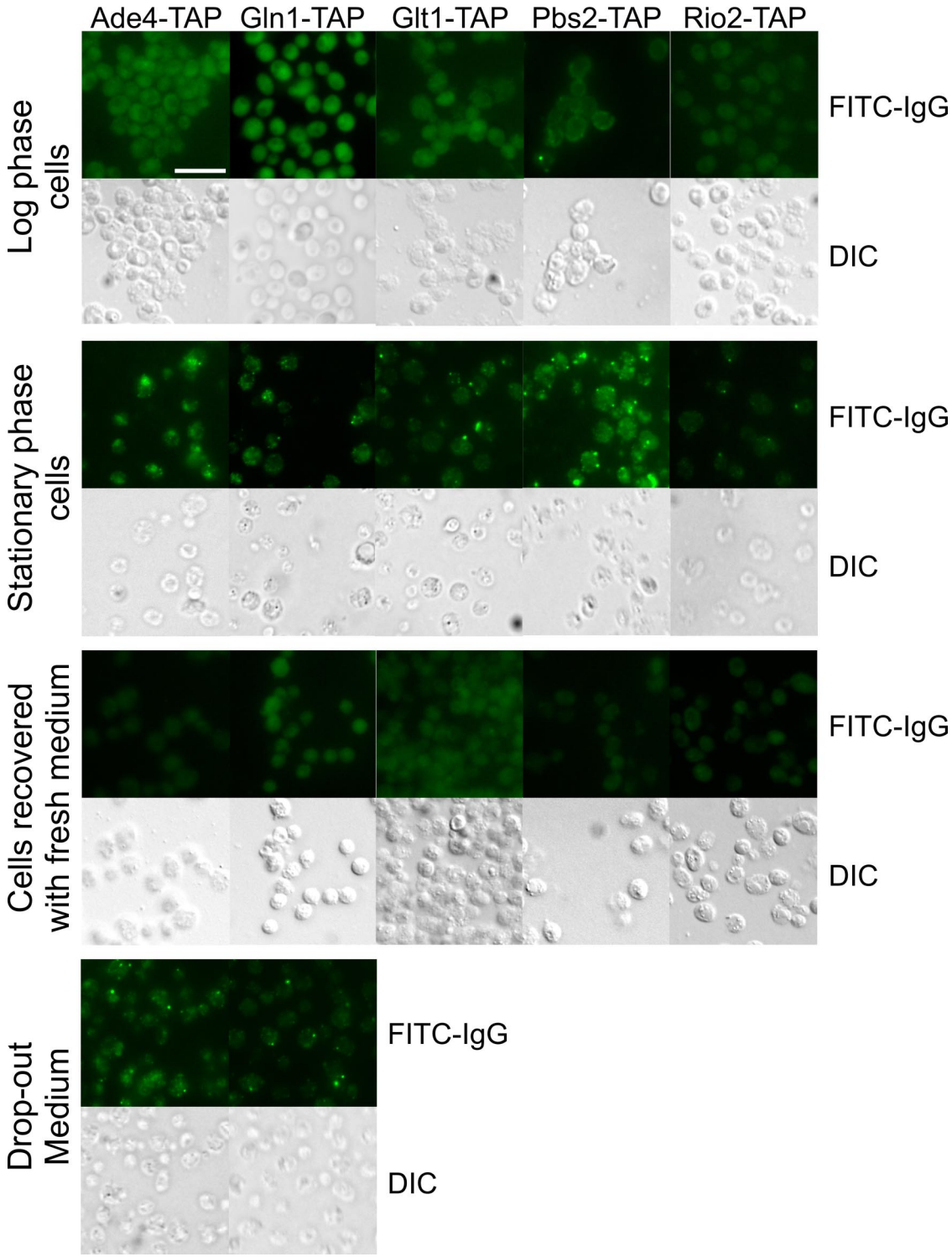

Fig. S4. Formation of punctate foci does not depend on presence of the GFP epitope tag, as measured by immunofluorescence observation of the foci formed by TAP-tagged Ade4, Gln1, Glt1, Pbs2, and Rio2 proteins. Like Ade4-GFP and Gln1-GFP, Ade4-TAP and Gln1-TAP show diffuse localization during log-phase growth and punctate foci in stationary phase cells or log-phase cells shifted into drop-out medium (SC-adenine or SC-glucose, respectively). Both proteins shift from punctate to diffuse state after readdition of fresh medium. Glt1, Pbs2, and Rio2 show the same trend. (Scale bar: 10 μm.)

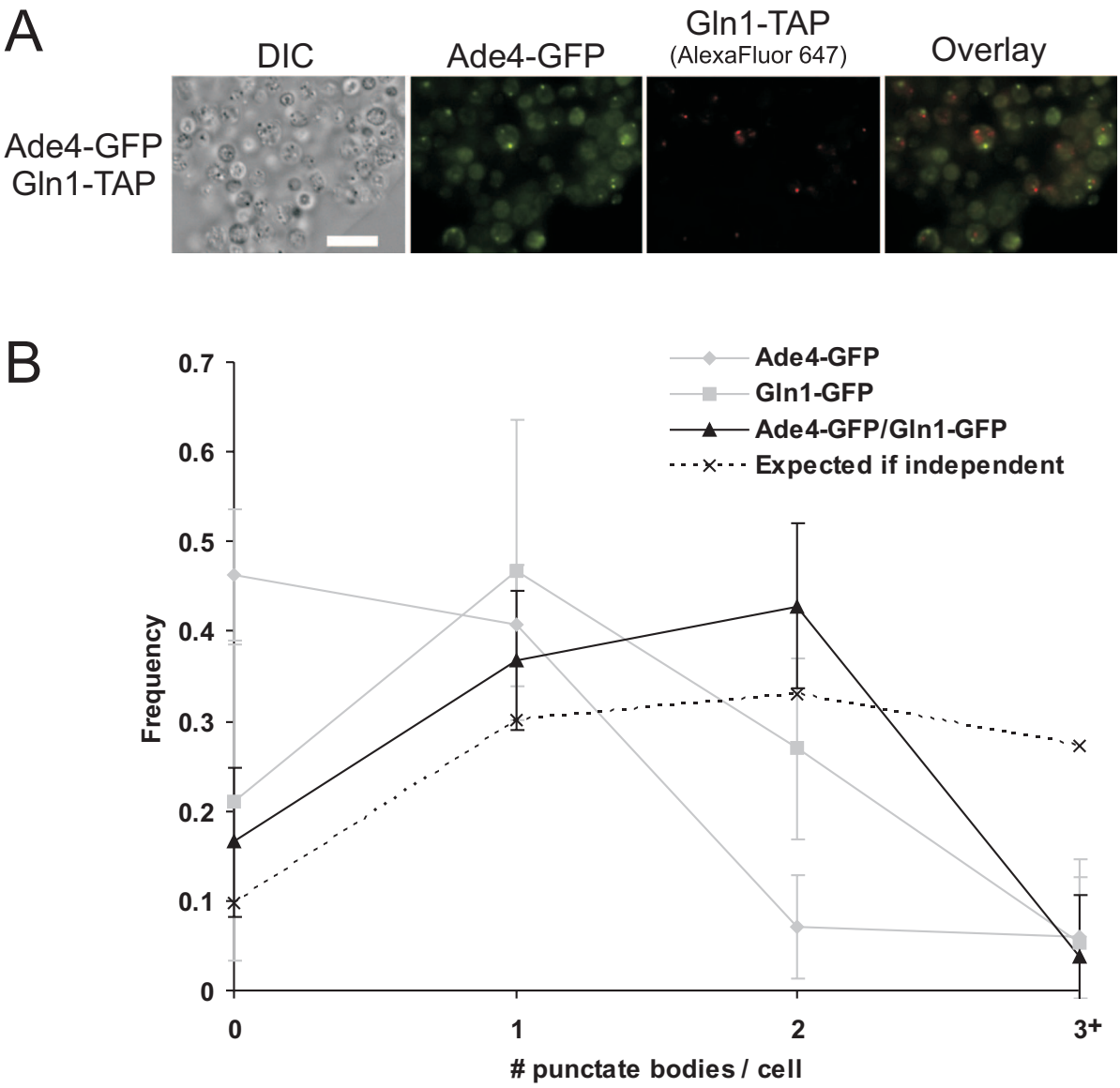

Fig. S5. (*A*) Ade4 and Gln1 punctate foci do not strongly colocalize with each other, as measured in a doubly-tagged strain by immunofluorescence observation of TAP-tagged Gln1 in a strain expressing GFP-tagged Ade4. Colocalization occurred in ≈2% of cells with both Ade4 and Gln1 foci (i.e., in 1 of 46 cells observed to express at least 1 punctate body of each type.) Cells were grown in SC medium for 48 h to stationary phase. (Scale bar: 10 μm.) (*B*) Additional evidence that Ade4 and Gln1 punctate foci do not strongly colocalize can be seen in the cell frequency histograms of punctate foci observed per cell for strains expressing Ade4-GFP, Gln1-GFP, or both. Strains expressing either Ade4-GFP or Gln1-GFP favor 1 punctate body per cell, whereas strains expressing both favor two, supporting the lack of colocalization and indicating that the GFP epitope tag is insufficient to direct aggregation specificity. Fewer cells with 3 or more punctate bodies were observed than expected, likely because of limited detection of fainter Ade4-GFP punctate bodies amid the general increase in background fluorescence accompanying expression of Gln1-GFP. Cells were grown in SC medium to early stationary phase. Error bars represent $\pm$1 SD, $n = 4$ biological replicates.

Other Supporting Information Files

Table S1

Table S2

Table S3

Dataset S1